Compact XFEL Schemes

Emmanuel d'Humières and Philippe Balcou
Université de Bordeaux – CEA - CNRS – CELIA, Bordeaux
France

1. Introduction

The quest for X-ray lasers has long been a major objective of laser science, starting from the early proposals of Duguay and Rentzepis, and of Jaeglé (2006), up to the modern large-scale projects of extreme UV and X-ray free electron lasers in Europe, Japan, Korea and the US.

X-ray radiation is one of the most efficient tools to explore the properties of matter in multidisciplinary domains. Over the past fifty years three generations of synchrotrons have been developed delivering x-ray beams with always shorter wavelength and higher brightness to a rapidly growing users community. These large scale instruments have lead to important discoveries and outstanding applications. However, while femtosecond x-ray pulses are now essential to open new possibilities of research and applications (Ultrafast Phenomena proceedings 1992-2002; Zewail 2000; Bloembergen et al., 1999; Rousse et al., 2001), the shortest pulse duration at synchrotron is a few tens picosecond. To face these technological limits, several methods have been proposed and demonstrated, based, for example on electron bunch slicing or Thomson scattering off a part of the bunch (Schoenlein et al., 1996 ; Schoenlein et al., 2000). However, these mechanisms are limited by their very low efficiency. Major progresses have been made with the fourth generation of synchrotron: the free electrons lasers (FEL). Even larger than a synchrotron, X-ray FELs can produce femtosecond x-ray pulses billion times more intense than any conventional source (Emma et al., 2010).

This continued effort, involving several scientific communities from laser physics, plasma physics, and accelerator physics, has already resulted in many experimental demonstrations of lasing, or of laser-like radiation, mostly in the extreme ultra-violet, or very soft Xray ranges. In the case of Xray lasers based on the interaction between intense laser pulses and plasmas, numerous lasing lines have been brought to saturation. High-harmonic generation, a process by which a femtosecond intense laser is converted directly into an XUV coherent beam, has bloomed into an extremely effective method for applications to time-resolved studies, down to the attosecond scale. In the field of laser-plasma interactions, incoherent X-ray sources obtained by shining an intense laser on plasmas or on free electrons have already allowed scientific premieres, such as sub-picosecond time-resolved diffraction studies of non thermal melting. Last but not least, the short-wavelength free electron lasers have recently achieved lasing, especially with the first X-ray light from the American LCLS (Emma et al., 2009). The European XFEL, and the Japanese SCSS projects will soon follow.

The impressive push to all those new technologies is not related to a problem of availability of X-ray sources, as the latter are readily available to the scientific and industrial

communities thanks to last generation synchrotron sources. However, a X-ray laser beam would possess inherently many novel properties, especially in terms of very short (femtosecond) time duration, and focusability to very small spots, thereby opening several new fields of research: single protein crystallography, strong field science in the X-rays, Warm Dense Matter, and even many medical applications, especially in oncology (Carroll 2003). The huge potential of all these applications was shown by the various scientific surveys performed to present the scientific cases of the major XFEL projects. Increasing the energy range of X-ray lasers beyond the current limit of roughly 10 keV for XFELs, would open even more numerous applications, and reaching the γ-ray range could even start brand new fields, such as nuclear laser spectroscopy.

However, the current XFEL projects are so large, both in size and budget, that they are bound to remain Large Scale Infrastructures, with a real issue of beam-time availability, and will not have the possibility to disseminate in university-scale research centers, industrial laboratories, or hospitals. The other technologies mentioned, such as laser-plasma X-ray lasers, high harmonic generation, Thomson (Inverse Compton) scattering on relativistic electrons, etc, are either too limited in flux, or simply restricted to the extreme ultra-violet wavelengths, and, while very useful for many studies, cannot be considered for some of the highest profile applications of XFELs.

Being able to combine the large flux and brilliance, and the operation in the real X-ray range of XFELs on one hand, and the compacity and reduced cost of XUV / X-ray sources derived from short pulse intense lasers on the other hand, would be an outstanding breakthrough in X-ray science. Facilities to generate X-ray pulses during the interaction of intense lasers and matter are compact, less costly, but yield mostly incoherent light, with low brightnesses. The development of coherent compact X-ray sources would allow to finally meet the current demand in X-ray sources for the applications discussed above.

Different setups are now considered, LINAC accelerated electrons coupled with a magnetic or an optical wiggler and laser wakefield accelerated electrons with a magnetic or an optical wiggler. Laser wakefield acceleration of electrons is increasingly considered as a potential compact substitute of conventional accelerator technology. It has made tremendous progresses in the last ten years thanks to the advent of short and high power Titane:Saphire systems. Two prospective schemes have recently being proposed with this goal, both based on the impressive progress of Laser WakeField Acceleration (LWFA) of electrons. On one hand, a few groups have proposed to use electron packets, accelerated in the LWFA or bubble regime up to energies around 1 GeV, and inject them into an undulator to obtain the micro-bunching effect of free electron lasers (Gruner et al., 2007). A second proposal revisits an old idea, which has remained so far inapplicable: the laser-undulator free electron laser (Petrillo et al., 2008). Both schemes are extremely interesting in the soft X-ray range around 1 keV. Both require however in a stringent way extremely challenging parameters of mono-energeticity and emittance of the laser-accelerated electron bunches. To the best of our knowledge, no compact scheme for an XFEL has yet been proposed, robust enough to be adapted to realistic conditions of relativistic electron bunches.

More recently, a new scheme using an all-optical setup has been proposed [P. Balcou et al. EPJD 2010]. It uses two counter-propagating lasers to create the wiggler and the X-ray radiation is created through a Raman scattering process between the electron bunching, the wiggler lasers and the generated X-rays.

We explore in this Chapter different opportunities to create a compact X-ray FEL, by coupling the physics of free electron lasers, of laser-plasma XUV lasers, and of extreme non-linear optics. In Section 2 the key physical mechanisms involved in these schemes are presented. In Section 3 several compact XFEL schemes proposed in the last twenty years are described. Section 4 is devoted to the recent proposal of a Raman compact XFEL and to a discussion on the possible parameters of an all-optical compact XFEL using this scheme. Section 5 closes this Chapter by discussing the perspectives of compact XFEL schemes.

2. Key physical mechanisms involved in these schemes

In this Section, the key physical mechanisms involved in the various compact XFEL schemes presented in this Chapter are discussed. First, the various techniques used to produce collimated energetic electron beams are reviewed. Then, magnetic and optical wigglers are presented and finally, the physics of electron beams trapped in an optical wiggler is discussed.

2.1 Energetic electron beam production

For the different compact XFEL schemes described below, a bunch of free electrons, with a kinetic energy in the range from 10 to 50 MeV, and hence a Lorentz factor from 20 to 100, needs to be produced using either a linear accelerator or a small high power short laser system. This element is typical of Thomson (inverse Compton) scattering experiments, or of free electron lasers, except for the use of smaller electron kinetic energies.

2.1.1 Linear particle accelerators

A linear particle accelerator (or LINAC) is a method of particle acceleration using oscillating electric potentials accelerating charged particles on a linear path. It was invented in the late 1920s. The design of a LINAC depends on the type of particles which it is supposed to accelerate and greatly varies in size depending on the energy the accelerated particles can reach (from a few meters to a few kilometers at SLAC in California).

In 1924, a theoretical paper by G. Ising, Stockholm, describes a method for accelerating positive ions (canal rays) by applying the electrical wavefront from a spark discharge to an array of drift tubes via transmission lines of successively greater lengths.

In 1928, an experimental paper (including the theory of betatron) by R. Wideroe, Switzerland, describes the successful acceleration of Potassium ions to 50 keV. The Potassium ions travel from one gap to the next one in one-half a radio frequency (RF) period. Since higher frequency oscillators did not exist at the time, lighter particles traveling faster could not be accelerated.

From 1931 to 1935, K. Kingdon (G.E.), L. Snoddy (Univ. of Virginia) et al., accelerate electrons from 28 keV to 2.5 MeV by applying progressive wavefronts to a drift tube array.

In 1947 and 1948, at Stanford, W. Hansen, E. Ginzton, W. Kennedy et al. build the Mark I disk-loaded LINAC yielding 4.5 MeV electrons in a nine-foot structure powered to 1 MW at 2856 MHz. It is the first of a series: Mark II (40 MeV), Mark III (1.2 GeV), and SLAC (30 GeV). Parallel efforts take place in Great Britain, France and the USSR, and at MIT and Yale in the USA.

In 1973, P. Wilson, D. Farkas and H. Hogg at SLAC invent the RF energy compression scheme called SLED which in the next five subsequent years gets installed on the 3-km LINAC, boosting its energy up to 30 GeV electrons.

A LINAC is composed of a particle source, a high voltage source for the initial injection of particles, a vacuum chamber containing electrically isolated cylindrical electrodes energized by sources of RF energy (Fig. 1). The frequency of the driving signal and the spacing of the gaps between electrodes are designed so that the maximum voltage difference appears as the particles crosses the gap. The particle velocity is therefore increased when it passes the gap and it is accelerated.

The disadvantages of LINACs are their length for devices designed to reach high energies, the associated power requirements and the fact that to reach high energies the device needs to be operated in bursts as the accelerating cavity walls can not sustain continuous heating.
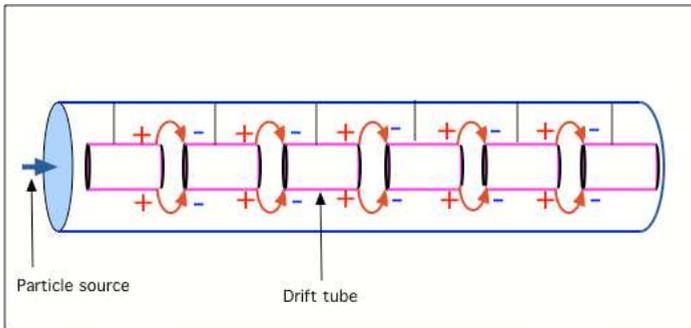

Fig. 1. Linear Particle Accelerator schematic.

Linear accelerators have made major contributions to physics research including neutron sources, colliding electron-positron beams, X-ray FELs, and heavy-ion rare-isotope beams. In addition electron linacs are used in hospitals around the world generating X-rays for radiation therapy, an application that represents one of the most significant spins-offs of high-energy and nuclear physics research.

Table 1 summarizes some industrial applications of RF LINACs with the associated characteristics. The LINACs are considered small devices.

		Favorable RF frequency
Electron beam processing - Sterilization - Polymer Reforming (< 10 MeV, > 10 kW)	High beam power	L-band S- band
Cargo inspection (3-9 MeV, ~1 kW)	↑ ↓	C-band
Radiotherapy (6-9 MeV, < 1 kW)	More compact	X-band

Table 1. Summary of industrial applications of RF LINACs.

The accelerating structure depends on the type of LINAC. The main types of LINACs are (Loew and Talman 1983):

- DC linacs, like Van de Graafs, in which the structure consists of a column of electrodes. These electrodes sustain a DC electric field which accelerates a continuous stream of particles. DC LINACs are limited to a few tens of MeV.
- Induction LINACs in which the accelerating electric fields are obtained, according to Faraday's law, from changing magnetic fluxes. These changing magnetic fluxes are generated by large pulsed currents driven through linear arrays of magnetic toroids. Induction LINACs are generally used in medium energy high-current pulsed applications.
- RF LINACs, either low frequency (UHF), microwave frequency (L, S, C, or X-band), laser frequency; CW or pulsed; traveling-wave or standing wave; room temperature or superconducting. In all these cases, the structure is a conducting array of gaps, cavities or gratings along which RF waves with an electric field parallel to the beam can be supported and built up through some resonant process. RF LINACs are used for a wide range of applications from injectors, to entire high-energy accelerators, medical accelerators.

For RF LINACs, the frequency of the driving oscillator is a crucial parameter. If a particle spends one RF cycle traveling between gaps, and the gap is small compared to the drift tubes. The distance between gaps, L, is then $L = \beta\lambda$, where $\beta = v/c$, c is the velocity of light, and λ is the RF wavelength. Note that the RF frequency is proportional to β. For a velocity ~c and a distance between gaps of a few cm, the frequency of the RF source ~GHz. High energy electron LINACs were, therefore, not possible until the development of high power microwave RF sources (Wilson, 2008). The relativistic relation between particle kinetic energy in electron volts, E_K, the rest energy E_0 and the normalized velocity is $E_K = E_0[(1 - \beta^2)^{-1/2} - 1]$. Here $E_0 = m_0c^2/e$, where e is the elementary charge and m_0 the electron rest mass. The difference between the relativistic and nonrelativistic regimes is approximately marked by a particle having an energy equal to its rest energy. For an electron this is an energy of 511 keV, while for a proton it is about 1 GeV. If electrons are injected at ~10 MeV, they can therefore be assumed to travel at c for design purposes.

2.1.2 Laser wakefield acceleration

In this section, a brief presentation of the principle and of the evolution of Laser Wakefield Acceleration of electrons is given. Different regimes of laser wakefield acceleration exists depending on the laser pulse duration, pulse width and intensity. The bubble regime of laser electron acceleration presented at the end of this section allows to produce quasi-monoenergetic electron beams with characteristics that make them very promising for XFEL applications.

Laser particle acceleration in vacuum is limited to the energy an electron can gain during a half laser period. With nowadays and even envisioned laser parameters, it will be difficult to reach energies higher than hundreds of MeV. Only a few experimental demonstrations of laser electron acceleration in vacuum exist, and the electron energies are lower than one MeV (Malka et al., 1997). It is possible to reach higher electron energies through resonance between the particle velocity and the wave phase velocity. The electromagnetic wave has a

super-luminous phase velocity and is not suited for particle acceleration. On the contrary, its group velocity in a plasma is lower than the velocity of light:

$$v_g = c\left(1 - \frac{n_e}{n_c}\right).$$

It depends on the ratio of the plasma electron density and the critical density: $n_c = \dfrac{m_e \omega^2 \varepsilon_0}{e^2}$.

Choosing the plasma density, it is easy to control the laser pulse group velocity and therefore the phase velocity of the plasma wave excited in its wake.

Plasma waves are adapted to accelerate electrons. The original idea was proposed by Tajima and Dawson in 1979 (Tajima and Dawson 1979). This mechanism consists of three steps – the excitation of a strong plasma wave using the laser pulse, the injection of electrons in the accelerating phase of the wave and the acceleration of electrons on a sufficient distance. The demonstration of plasma waves generated by laser pulses was obtained experimentally at the end of the eighties and electron beams accelerated in plasma waves nowadays reach energies higher than a GeV (Leemans et al., 2006).

Linear regime - The plasma wave is excited during the propagation of a laser pulse in an underdense plasma, $n_e \ll n_c$, by the ponderomotive force (see Fig. 2). The plasma density defines the plasma wave pulsation, ω_{pe}, whereas the pulse velocity defines its phase velocity, $v_{ph} = \omega_{pe}/k_p = v_g$. The wave vector can therefore be written:

$$k_p = \frac{\omega_{pe}}{c}\left(1 - \frac{\omega_{pe}^2}{\omega^2}\right)^{-1/2} = \frac{\omega}{\gamma_p \beta_p c}$$

Where we have introduced the relativistic factor of the plasma wave, $\gamma_p = \left(1 - \beta_p^2\right)^{-1/2} = \omega / \omega_{pe}$, and $\beta_p = \sqrt{1 - n_e / n_c}$. Moreover, in a low density plasma, the plasma wave is strongly relativistic, $\gamma_p \gg 1$, and its wavelength is γ_p times higher than the laser wavelength.

The amplitude of the plasma wave depends on the laser pulse amplitude and on its duration τ_0. The most advantageous case is for $\tau_0 \omega_{pe} \sim 1$ when the electrostatic potential of the plasma wave is $\psi_p \sim a^2 m_e c^2$, where a=eE/(m$_e$cω). The amplitude of the electron density perturbation, $\delta n_e / n_e \sim a^2$, is therefore directly proportional to the laser intensity. For relativistic laser pulses, the plasma wave becomes strongly non-linear, the electrons accumulate in front of the laser pulse whereas an excess of ions if formed behind the laser pulse.

To have a more complete vision, it is necessary to take into account the laser pulse radius in the direction perpendicular to the propagation axis. If the laser radius w_0 is small compared to the electron inertia length, $w_0 < c / \omega_{pe} = 1 / k_p$, the laser pulse diffracts rapidly on the Rayleigh length $z_R = \frac{1}{2} k w_0^2$ which is not sufficient to create an efficient wakefield. On the contrary, for large pulse radii, $k_p w_0 > 1$, filamentation and self-guiding of the laser pulse can occur.
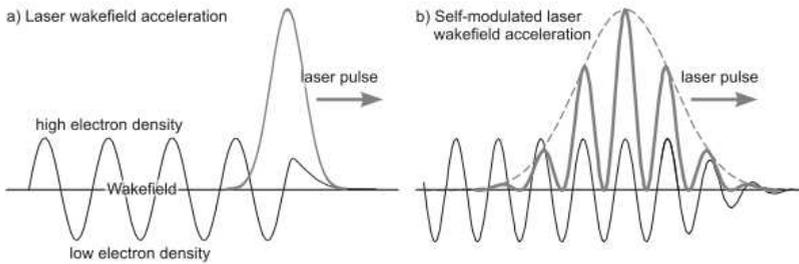
Fig. 2. Laser eneveloppe and electron density schematic in the laser wakefield regime (a) and in the self-modulated wakefield regime.

The relativistic self-guiding threshold power is given by the formula $P_c = 8\pi n_c m_e c^5 / \omega_{pe}^2$ (Gibbon 2005). The condition on laser power $P = P_c$ in dimensionless units corresponds to the condition $a^2 k_p w_0^2 = 8$ and therefore the wakefield excitation occurs at the same time as the laser pulse self-guiding. Self-guiding is indeed desirable to guide the pulse on a distance of several Rayleigh lengths. The guiding criteria qualitatively comes from the condition that the radial pronderomotive force, $f_p \sim a m_e c^2 / w_0$, is balanced by the attraction force acting on electrons due to the ions electrostatic field, $eE_r \sim m_e \omega_{pe}^2 w_0$. The equilibrium criterion is then $k_p w_0 \sim 2\sqrt{a}$. The factor 2 in this formula was obtained in (Lu et al. 2007) using numerical simulations.

Beat wave - Initially, laser pulses had pulse durations longer than the plasma period. To couple more efficiently the laser pulse with the plasma wave, a technique had to be developed to generate an electromagnetic wave at the plasma frequency. This mechanism requires two counterpropagating pulses with pulsations ω_1 and ω_2 chosen so their difference corresponds to the plasma pulsation $\omega_2 - \omega_1 = \omega_{pe}$.

The superposition of these two pulses therefore produces a beat wave at ω_{pe} that excites resonantly the plasma wave. The amplitude of the plasma wave reaches about 30% of the initial density in this regime, which limits the accelerating field to a few GV/m.

In 1993, Clayton et al. (Clayton et al., 1994) obtained a final energy of 9.1 MeV for injected electrons energies of 2.1 MeV. Experiments in this regime were also conducted at UCLA (Everett et al., 1994) (gain of 30 MeV), at Ecole Polytechnique (Amiranoff et al., 1995) and at Osaka (Kitagawa et al., 1992) for instance.

The physical mechanisms limiting this technique are the ions movement, which needs to be taken into account for such high pulse durations, the relativistic dephasing of the plasma wave for higher laser intensities and the growth of instabilities.

Non-linear regimes - Self-modulated wakefield - With the advent of laser systems with high laser intensity, shorter pulse durations (500fs) and high energy (100J), plasma non-linear effects could be studied. The cumulated effects of self-guiding and self-modulation of the laser envelope with the perturbation of the initial electron density generate a laser pulse train which resonates with the plasma wave. These effects are presented in Fig. 2. The self-modulated wakefield mechanisms has first been studied theoretically (Sprangle et al., 1992; Antonsen and Mora, 1992; Andreev et al., 1992). These studies show that when the pulse

duration his higher than the plasma period and when the laser power is higher than the self-guiding critical power, a unique laser pulse is modulated at the plasma wavelength during its propagation. This mechanism, designated as Raman scattering and that describes the decomposition of an electromagnetic wave in a plasma wave and another electromagnetic wave shifted in frequency, leads to a modulation similar to the ones obtained by the wave beating mechanism using two laser pulses and produces energetic electrons (Joshi et al., 1981).
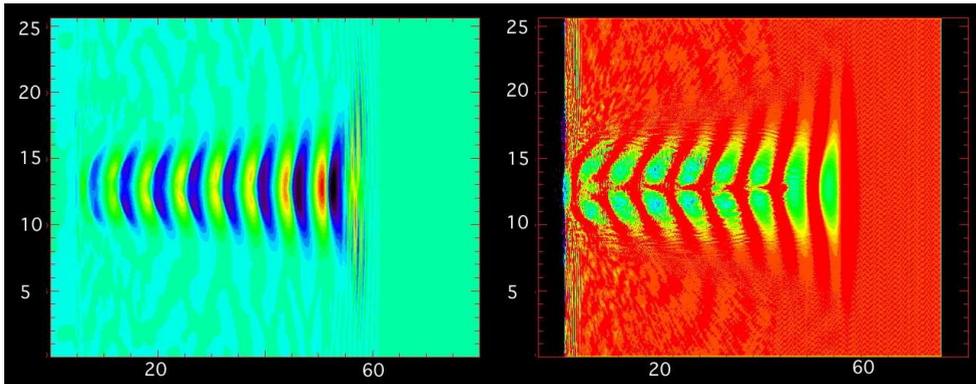

Fig. 3. 2D Particle-In-Cell simulation results of the propagation of a high intensity laser in a low density plasma. (a) Electric field in the propagation direction. (b) Electron density map. Axis are in wavelengths. Laser intensity is 4.3×10^{18} W/cm^2 and pulse duration is 10 fs. Laser FWHM is 3 wavelengths. Plasma density is 0.02533 n_c and plasma length is 80 wavelengths.
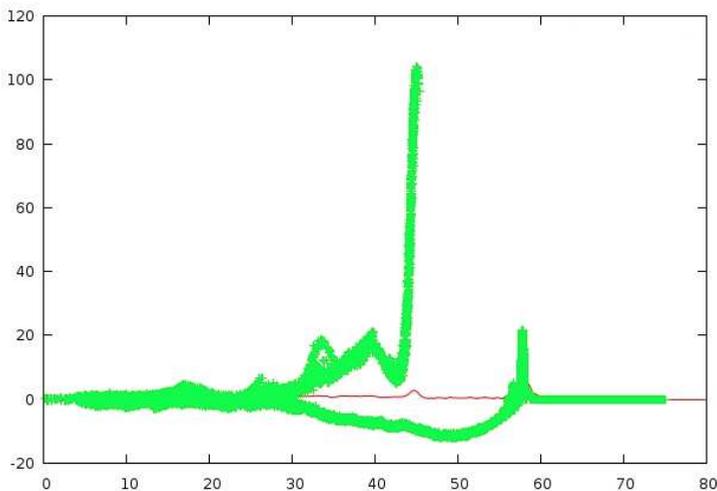

Fig. 4. 1D Particle-In-Cell simulation results of the propagation of a high intensity laser in a low density plasma. Electron phase space at t=198 fs. Laser intensity is 1.7×10^{19} W/cm^2 and pulse duration is 10 fs. Plasma density is 0.02533 n_c and plasma length is 80 wavelengths. Y-axis corresponds to $\beta\gamma$ and x-axis is in wavelengths.

Forced wakefield - Thanks to the advent of the Chirped Pulse Amplification technique [Strickland and Mourou 1985], the new properties of high intensity laser interaction with matter, typically experimented on big laser facilities, became accessible to smaller laser systems adapted to the academic community. These systems, most using Titane Sapphire crystals, fit in a room of a few square meters and deliver an energy of about 2-3 J in 20 fs on target. This corresponds to lasers of the 100 TW class with focalized intensities of the order of a few 10^{19} W/cm². Numerous publications have shown that these moderate energies installations, working at a high repetition rate of 10 Hz and of a reasonable price can produce energetic electron beams of very high quality. For example, using the "Salle Jaune" laser at LOA in France, electrons were accelerated up to 200 MeV in 3 mm of plasma (Malka et al., 2002). The accelerating mechanism is called forced wakefield to distinguish it from the self-modulated wakefield mechanism (see Fig. 2). Indeed, using short duration laser pulses, plasma heating in the forced wakefield regime is less important than in the self-modulated regime. This allows reaching higher plasma wave amplitudes and therefore high electron energies. Thanks to shorter interaction duration between the laser and the accelerated electrons, the electron beam quality is also enhanced. The measure of the normalized transverse emittance gives comparable values as conventional accelerators with similar energies (rms normalized emittance of 3π mm·mrad for electrons with an energy of 55 ± 2 MeV) (Fritzler et al., 2004). Electron beams with maxwellian spectral distributions, generated using ultra short laser pulses, were obtained in several laboratories around the world: at LBNL (Leemans et al., 2004), at NERL (Hosokai et al., 2003), and in Europe at LOA in France (Malka et al., 2001) or at MPQ in Germany (Gahn et al., 1999) for example. Figure 3 shows the results of a 2D Particle-In-Cell simulation of the propagation of a high intensity pulse in a low density plasma leading to the creation of a plasma wave and strong electrostatic fields. Figure 4 shows the electron phase space in a 1D simulation with similar interaction parameters leading to the production of a broad electron energy spectrum with maximum energies higher than 50 MeV.

The previous regimes are limited by non-linear effects of which wavebreaking is one of the most important. The maximum electric field that a plasma wave can sustain is limited by wave breaking. This wave breaking takes place when the electrons participating to the plasma wave are trapped in the wave itself and then accelerated. This leads to the loss of structure of the electrons generating the electric field of the wave, and therefore to the damping of its amplitude. For a relativistic plasma wave, the electric field when wave breaking starts is (Arkhiezer and Polovin, 1956): $E_{break} = \sqrt{2(\gamma_p - 1)}E_0$, where $E_0 = m_e c \omega_{pe} / e$.

This formula is obtained in the cold plasma limit. Thermal effects will launch wave breaking before the cold wave breaking limit (Rosenzweig, 1988; Katsouleas and Mori, 1988).

Bubble regime - More recently, theoretical works based on 3D Particle-In-Cell simulations have shown the existence of a robust acceleration scheme called the bubble regime (Pukhov and Meyer-ter Vehn, 2002). In this regime, the laser dimensions are shorter than the plasma wavelength in the longitudinal direction but also in the transverse directions. The laser pulse therefore resembles a light sphere with a radius smaller than 10 μm. If the laser energy contained in this volume is sufficiently high, the laser ponderomotive force efficiently expels radially plasma electrons, creating an electronless cavity behind the laser pulse, surrounded by a dense electron zone. The total expulsion of electrons was predicted in numerical

simulations (Pukhov and Meyer-ter-Vehn 2002) and two years later, it was observed in experiments (Faure et al. 2004). The electrons expelled by the laser glide around the cavity (see Fig. 5) and some of them enter the cavity from the back. Some electrons are injected in the cavity and accelerated along the laser axis, producing an electron beam with radial and longitudinal dimensions smaller than the laser dimensions (see Fig. 5). The details of the electron injection process are not yet completely understood, but it is observed in several simulations that are in good agreement with experiments. A new electron injection technique using a secondary laser has recently been demonstrated experimentally (Faure et al., 2006).
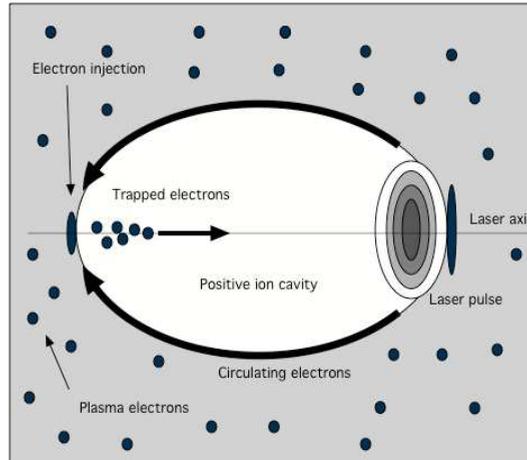

Fig. 5. Schematic of the bubble regime of laser electron acceleration in low density plasmas.

The signature of this regime is a quasi-monoenergetic electron distribution. This property differs significantly from previous results on laser electron acceleration. It comes from the combination of several factors:

- Electron injection in the cavity is different from the injection linked to wavebreaking in the self-modulated and forced wakefield regimes. The injection does not originate from the "breaking" of the accelerating structure. It is located at the back of the cavity, which gives similar properties to injected electrons in the phase space.
- Acceleration occurs in the stable accelerating structure during the propagation as long as laser intensity is sufficiently high.
- Electrons are trapped behind the laser, which limits the interaction with the laser transverse electric field. Trapping stops when the charge contained inside the cavity compensates the ion charge.
- Rotation of electrons in the phase space also contributes to reduce the spectral width of electron bunches (Tsung et al., 2004).

As soon as an electron enters the cavity, it is attracted to the center by the ion electrostatic field. At the same time, the electric field focalizes the electron towards the laser axis. The value of this accelerating force has already been estimated above:

$$eE_r \sim m_e \omega_{pe} c \sqrt{a}$$

A magnetic field also exists inside the cavity. It originates from the fact that the cavity glides on fixed ions creating a current density $-en_e c \beta_p$ in the direction opposite to the propagation direction. The amplitude of this field is proportional to the distance to the center of the cavity and its maximum value is:

$$eB_\varphi \sim m_e \omega_{pe} \sqrt{a}$$

so that the Lorentz force is equal to the electrostatic force.

We can now estimate the maximum energy that an electron can gain inside the cavity. In the reference frame of the cavity, it is stretched in the propagation direction by the factor γ_p. Therefore, the electron energy gain in the cavity $\varepsilon'_e \sim m_e c^2 \gamma_p a$ is the product of the electric force $\sim m_e \omega_{pe} c \sqrt{a}$ and the acceleration length $\gamma_p \sqrt{a} / k_p$. It is then necessary to multiply this result by the factor γ_p to come back to the ion reference frame. The final energy of an accelerated electron is therefore:

$$\varepsilon_e \sim m_e c^2 \gamma_p^2 a = m_e c^2 a \frac{\omega^2}{\omega_{pe}^2}$$

It is proportional to the laser field amplitude and moreover it is inversely proportional to the plasma density.

It is therefore better to work with moderate laser intensities, a~5 and to use low density plasmas with densities $\leq 10^{18}$ cm^{-3} to reach GeV electron energies. Nevertheless, the increase of the electron energy also requires a longer acceleration length. The length travelled by the electron in the laboratory reference frame during its acceleration is:

$$l_{acc} \sim \frac{R}{1 - \beta_p} \sim \frac{c}{\omega} \gamma_p^3 \sqrt{a}$$

It strongly increases with the energy gain and self-guiding of the laser pulse beyond a few mm seems difficult.

Several laboratories have obtained electron bunches with quasi-monoenergetic spectra: in France (Faure et al. 2004) with laser pulses duration shorter than the plasma period, but also using laser pulses longer than the plasma period in the United Kingdom (Mangles et al. 2004), and in the US (Geddes et al., 2004), then in Japan (Miura et al. 2005) and in Germany (Hidding et al., 2006). There is great interest in such beams for applications: it is now possible to transport and refocalize this beam using magnetic elements. With a maxwellian spectrum, it would have been necessary to select an energy range for transport, which would have strongly decreased the electron flux.

Future of laser electron acceleration - Some solutions are now proposed to reach energies of several GeVs. It is possible to increase the acceleration length by guiding the laser pulse either using a capillary filled with gas (Leemans et al. 2006) or by tuning properly laser and plasma parameters (Hafz et al., 2008). Nevertheless, acceleration using multiple stages seems necessary to go further. The first demonstrations of electron acceleration in two stages were reported (Liu et al., 2011 ; Pollock et al., 2011). Counter-propagating lasers to separate

the wake creation and the injection mechanism lead to a better reproducibility with a good quasi-monoenergeticity (J. Faure et al. 2006, Davoine et al 2009). This scheme is designated as controlled optical injection. Bunch duration was also measured at LOA, France (O. Lundh 2011). Their analysis shows that the electron beam, produced using controlled optical injection, contains a temporal feature that can be identified as a 15 pC, 1.4–1.8 fs electron bunch (root mean square) leading to a peak current of 3–4 kA depending on the bunch shape.

For the XFEL compact schemes application, the maximum electron energy is not the most important parameter. Reaching better emittance with smaller energy spread is the goal. Table 2 summarizes some important parameters of electron beams accelerated either by LINACs or by laser wakefield acceleration.

	Typical energy	Energy spread	Beam intensity	Emittance
LINAC (CERN LINAC96 compendium)	30-100 MeV	0.5-3 %	0.1-70 A	0.2-100 mm·mrad
Laser electron acceleration (X. Davoine et al. 2009)	60 MeV	1-2 %	25 kA	1 mm·mrad

Table 2. Summary of some important parameters of electron beams accelerated either by LINACs or by laser wakefield acceleration

As shown in Table 2, the main advantage of laser wakefield acceleration is in the very high achievable beam intensities. It is important to note that this table does not include parameters of very high energy LINACs which are out of the scope of this Chapter.

2.2 Wigglers (magnetic and optical)

2.2.1 Magnetic wigglers

Coherent emission by an electron beam in a FEL relies upon the self-consistent interaction between the electrons and radiation as the electron beam undulates in the magnetic undulator field. The undulator and resonant electromagnetic fields form a ponderomotive potential which co-propagates at the mean electron velocity along the axis of the undulator (Winick et al., 1981). The relativistic electron beam is bunched by this potential and forms a periodic density modulation at the resonant radiation wavelength (see Fig. 6). Emission from the electron beam is therefore coherent and may be many orders of magnitude greater than the incoherent emission from a similar, but unbunched, beam.

1D models of the FEL interaction between a pulse of electrons and a linearly-polarized radiation field in a planar undulator FEL are widely used. In deriving the equations that describe the FEL interaction, it is possible to neglect explicit three-dimensional effects such as electron beam emittance and radiation diffraction. These effects may be re-introduced into the reduced one-dimensional model by using further approximations. When three-dimensional effects are included in FEL models they generally tend to degrade the quality of the FEL interaction by reducing saturation powers and decreasing the radiation gain per unit length. The one-dimensional FEL model is therefore the 'best-case' model for a given set of parameters.
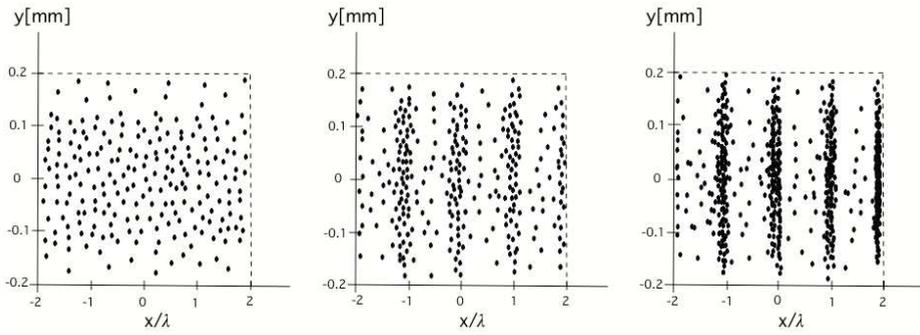
Fig. 6. Schematic of the bunching of electrons in a magnetic undulator.

A magnetic wiggler is characterized by its undulator parameter $K=eB_0\lambda_u/(2\pi m_e c)$. λ_u is the wiggler wavelength and B_0 is its magnetic field amplitude (Lau et al., 2003). Synchrotron radiation is emitted inside a cone with opening angle $1/\gamma$. If $K \leq 1$, the electron trajectory is inside the radiation cone. Therefore, the photons emitted by an electron at various positions interfere with each other. The radiation is therefore monochromatic. the wavelength of the undulator light is given by $\lambda = \lambda_u/2\gamma^2(1 + K^2/2)$. The essential feature of the high-gain FEL is that a large number of electrons radiate coherently. In that case, the intensity of the radiation field grows quadratically with the number of particles: $I \sim N^2$. More information on magnetic wigglers can be found in other chapters of this book.

2.2.2 Optical wigglers

Many authors have shown that the action of a laser field, counter-propagating with respect to the electrons, is basically equivalent to that of the magnetic field in a wiggler, and thus can be used to obtain an FEL effect (Sprangle 2009b ; Dobiasch et al., 1983 ; Gea-Banacloche et al, 1987; Gallardo et al., 1988). In fact, the laser parameter a is found to be almost interchangeable with the FEL wiggler parameter K. Many realistic effects that have been studied in the conventional synchrotron/FEL community may be immediately applied to the laser synchrotron. However, the strength parameter K depends strongly on the undulator period. Replacing the magnet period of few cm, by a laser wavelength around 1 μm, results in practice in a very low value of K, and hence in low gain, so that a very high number N of oscillations is required.

Another way to produce an optical wiggler is to use multiple lasers to generate an optical lattice. An optical lattice is formed by the interference of counter-propagating laser beams. The beam interaction produces a spatially periodic potential. One of its uses is to trap neutral cooled atoms at the locations of potential minima in atomic physics (three laser beams for the optical molasses technique) and to produce Bose-Einstein condensates. The advantage on magneto-optical traps is the periodicity induced in the cold atomic gases, making it alike a solid crystal.

Using two counter-propagating laser beams, it is possible to create a ponderomotive potential array. Kapitza and Dirac (1933) have shown that electrons interacting with a light standing wave can diffract from this light lattice – thus undergoing the reverse process of light diffraction on a matter density grating. In the low intensity limit, the interaction with the light is a small perturbation to the electron free motion, that induces a momentum

transfer of $\pm(h/\pi)k$, where h is the Planck constant and k is the wavevector of either beam forming the standing wave (D.L. Freimund et al., 2001). Conversely, at high intensities of the order of 10^{13} W/cm2 or more for near infrared lasers, the electron dynamics is modified considerably by the action of the light lattice. Free electrons interacting with a spatially non uniform laser field are indeed submitted to a significant ponderomotive force, i.e., a drift force tending to expel the electrons from the regions of highest intensity (Kibble 1968). Free electrons are in effect embedded into a spatially varying potential induced by light, resembling a series of parallel half-pipes. This situation is extremely similar to that of optical molasses, well-known in the field of cold atoms, that play for instance a role in Sisyphus cooling. Giant momentum exchanges of several 10^3 $(h/2\pi)k$ or more can be induced; at such levels, the quantum description of electrons becomes useless, and a classical description is valid. The existence of the strong field Kapitza-Dirac effect has been demonstrated experimentally by Bucksbaum et al. (1988), and briefly rewieved by Hartemann (2000). Interaction of relativistic electrons and a standing wave in the strong field KD regime has only been briefly considered by Fedorov et al. (1988).

2.2.3 Raman FEL lasers: From Raman to Compton regimes of FEL emission

The low-gain, tenuous-beam limit is relevant to free-electron laser configurations in which the electron beam current is low and the gain of the signal in a single pass is less than unity. In the linear theory of this regime, the beam plasma frequency $\omega_b \ll \omega$ and collective effects due to beam space-charge waves are negligible. The high-gain regime is applicable to intense-beam FELs. The fields in this regime exhibit exponential growth of the fluctuation fields. The wiggler field provides for the coupling between the beam space-charge wave and either polarization state of the electromagnetic field, as well as a growth mechanism for the electromagnetic waves in the absence of the beam-plasma waves (Freund and Antonsen, 1996). In the former case, coherent amplification occurs by three-wave coherent Raman scattering in which the wiggler represents the pump wave, the beam-plasma wave mode represents the idler, and the output signal is the daughter wave. The latter case is coherent Compton scattering in which the wiggler scatters off the electron beam. There are two principal regimes of interest in the solution of the dispersion equation corresponding to the low- and high-density regimes. The high-gain Compton regime is achieved when the ponderomotive potential is larger than the space-charge potential of the beam-plasma waves. The opposite case in which the space-charge potential is larger than the ponderomotive potential is the Raman regime. In the Compton regime, the electron beam interacts with the ponderomotive potential formed by the beating of the wiggler and radiation fields. For high currents, the electrostatic potential due to the beam space-charge waves is dominant, and the interaction leads to stimulated Raman scattering of the space-charge wave off the wiggler. An intermediate regime exists in which both mechanisms are operative.

2.3 Behaviour of free electrons in relativistic laser fields

2.3.1 Electron motion in an electromagnetic field

This motion is described by Newton's equation with Lorentz force. Electric and magnetic field are given by Maxwell's equations. To use these equations in an invariant form, it is better to use the vector potential $\vec{A}$ in Coulomb's gauge. The equation of motion of the electron is then:

$$d_t \vec{p} = e \partial_t \vec{A} + e(\vec{v} \cdot \nabla) \vec{A} - e \nabla (\vec{v} \cdot \vec{A}) \tag{1}$$

Considering a plane electromagnetic wave propagating in the z direction, $\vec{A}_\perp(z,t)$, we can decompose this equation in two components. In the direction perpendicular to the propagation direction, $d_t \vec{p}_\perp = e \partial_t \vec{A}_\perp + e v_{//} \partial_z \vec{A}_\perp \equiv e d_t \vec{A}_\perp (z_e(t),t)$, where $z_e(t) = \int_t v_{//} dt$. This relation gives the conservation of generalized momentum $\vec{P}_\perp = \vec{p}_\perp - e \vec{A}_\perp$ and for an electron initially at rest, $\vec{p}_\perp = e \vec{A}_\perp (z_e(t),t)$. It is a direct consequence of the fact that the wave is homogeneous in the x and y directions.

In the direction parallel to the propagation direction, Eq. 1 gives: $d_t p_{//} = -\dfrac{e}{m_e \gamma} \vec{p}_\perp \cdot \partial_z \vec{A}_\perp$, and using the conservation of generalized momentum:

$$d_t p_{//} = -\frac{e^2}{2 m_e \gamma} \partial_z \vec{A}_\perp^{\ 2} \tag{2}$$

γ is the relativistic factor of the electron. The kinetic energy of the electron is $\varepsilon = (\gamma - 1) m_e c^2$ and the velocity of the electron is related to its energy by $\vec{v} = \partial_{\vec{p}} \varepsilon$, leading to:

$$d_t \varepsilon = e \vec{v} \cdot \partial_t \vec{A} \tag{3}$$

Using Eq. 2 and Eq. 3 leads to:

$$d_t \left[(\gamma - 1) m_e c^2 - p_{//} c \right] = \frac{e^2}{2 m_e \gamma} (\partial_t + c \partial_z) \vec{A}_\perp^{\ 2} \tag{4}$$

For a progressive wave propagating at the velocity c, the vector potential is a function of the variable t-z/c and the right side of Eq. 4 is equal to zero. The conservation of the parallel momentum is therefore obtained and for a particle initially at rest:

$$p_{//} = m_e c (\gamma - 1) \tag{5}$$

A relation between parallel and perpendicular components of the momentum is therefore also obtained:

$$p_{//} = \frac{\vec{p}_\perp^2}{2 m_e c} \tag{6}$$

After the wave has passed, the electron is again at rest. The sign of the parallel momentum is always positive meaning that the electron is pushed by the wave in its propagation direction.

From Eq. 5 and Eq. 6, it is also possible to deduce the divergence angle of the electron and its link with the particle energy:

$$\tan \theta = \frac{p_\perp}{p_{//}} = \sqrt{\frac{2}{\gamma - 1}} \tag{7}$$

Relativistic electrons are therefore ejected in the propagation direction, whereas non-relativistic electrons are ejected in the polarization direction.

To study in more detail the trajectories of the electrons in the wave, we can use the proper time $\tau = t - z_e(t)/c$ to get a linear equation for the orbit of the particle:

$$\frac{d\vec{r}_e}{d\tau} = \gamma\vec{v} = \frac{\vec{p}}{m_e} \tag{8}$$

For a linearly polarized wave, $\vec{A}_\perp(z,t) = (m_e c / e) a\cos(\omega\tau)\vec{e}_x$, one can obtain:

$$kx_e(t) = a\sin(\omega\tau), kz_e(t) = \frac{a^2}{8}(2\omega\tau + \sin(2\omega\tau)).$$

The simple motion in the perpendicular plane comes with a more complicated motion in the propagation direction of the wave. It is periodical but it is not a sinusoid. It also contains several harmonics of the wave frequency. In the non-relativistic regime, the main harmonic is dominant. In the relativistic regime, the number of harmonics becomes important.
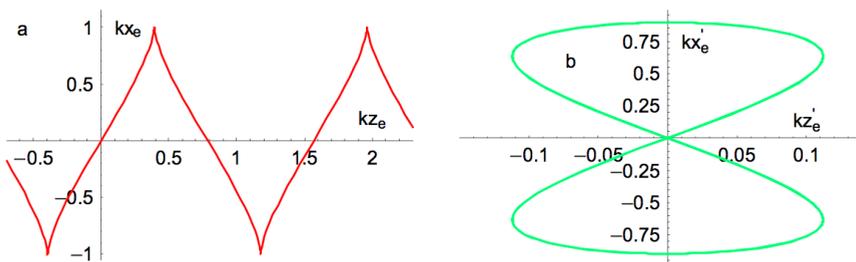

Fig. 7. Orbit of an electron in the (x,z) plane due to a linearly polarized progressive electromagnetic wave: (a) in the laboratory reference frame and (b) in the reference frame moving at the particle drift velocity. The dimensionless amplitude of the wave is a=1.

An example of the orbit of an electron in a linearly polarized wave is shown in Fig. 7. In the reference frame of the laboratory, maximum velocity is achieved when x_e is close to zero, and the orbit is peaked for large values of x_e, when acceleration is at its maximum. The shape of this orbit is more simple in the reference frame moving at the drift velocity of the article v_d in the z direction as it becomes closed. It is the well-known "figure eight". v_d is given by $a^2c/(a^2+4)$.

2.3.2 Relativistic ponderomotive force

The force on the right side of Eq. 2 is proportional to the square of the laser pulse amplitude. It therefore contains an average component and an oscillating component with a period of π/ω, the laser pulse half-period. The average part of this force is the ponderomotive force. It acts on all charged particles (but mostly on electrons due to their small mass) and it pushes particles independently of the sign of their charge in the direction opposed to the intensity gradient. A more general expression of Eq. 6 for the average part of the momentum is:

$$d_t(p) = f_p \equiv -\frac{e^2}{2m_e(\gamma)}\nabla\left(\vec{A}^2\right)$$ (9)

The averaging is done over a laser period. The average relativistic factor is given by:

$$(\gamma) = \sqrt{1 + \frac{(\vec{p})^2}{m_e^2 c^2} + \frac{e^2\left(\vec{A}^2\right)}{m_e^2 c^2}}$$

It takes into account the average momentum $(\vec{p})$ and the oscillating momentum $\vec{p}_{osc} = e\vec{A}$. The ponderomotive force in Eq. 9 can be presented in a more simple expression, noting that in (γ), only the oscillating part depends on coordinates, while the average momentum $(\vec{p})$ is a function of time. The ponderomotive force can therefore be written:

$$f_p = -m_e c^2 \nabla(\gamma).$$

The importance of this latest expression comes from the fact that the ponderomotive force is presented as the gradient of the ponderomotive potential, $U_p = m_e c^2\left((\gamma)-1\right)$. As for all potential forces, the work of the ponderomotive force does not depend on the particle trajectory but only on the starting and on the ending points. It gives another interpretation of the fact that a free charged particle cannot gain (or lose) kinetic energy in the laser pulse. It is the Lawson-Woodward theorem. Even if this theorem is verified in the ideal case described above, several possibilities exist for the electron to gain energy in the wave.

2.3.3 Nonlinear Thomson scattering

In Thomson scattering, an electron that is initially at rest may acquire relativistic velocities in the fields of high-intensity light and emit radiation at high harmonics of the light frequency. If the electron already possesses a relativistic energy before it encounters the high-intensity laser, there is an additional Doppler-shift of the scattered light.

For lasers with low intensities (a<<1), an electron that is initially at rest undergoes a small amplitude, transverse oscillation at the laser frequency. The Thomson scattering spectrum consists of a single frequency in all directions and the radiation pattern is the same as that from a dipole. If a is increased to a few tens of percent, the electron's oscillation frequency begins to deviate from the laser frequency (see Lau et al., 2003). If a~1, the Lorentz force associated with the laser's magnetic field becomes significant, and the electron acquires an oscillation along the laser propagation direction, in addition to the transverse oscillation (see Section 2.3.2). The electron also acquires an average drift velocity along k. For a>>1, the axial oscillation greatly exceeds the transverse oscillation, and the electron orbital period is much greater than the laser optical period. A non-linear scattering spectrum is therefore obtained.

The tutorial given on this regime in (Lau et al. 2003) is based on the simple, classical model of a single electron interacting with an infinite plane wave. While highly idealized, it suggests that the brightest x-ray source is achieved by head-on collisions of a relativistic electron beam with an intense laser with a>1. Such a configuration, broadly known as laser synchrotron, strongly resembles the conventional synchrotron/FEL.

3. Description of existing FEL compact schemes

3.1 LWFA coupled with a magnetic wiggler

A few groups have proposed to use electron packets, accelerated in the LWFA or bubble regime up to energies around 1 GeV, and inject them into an undulator to obtain the micro-bunching effect of free electron lasers (Grüner et al., 2007). This would result in a XUV or soft X-ray source, in the 1 keV range; an important hurdle is the effect of space charge, that induces a large expansion of the accelerated electron bunch within the wiggler, and might limit the amplification.

Laser wakefield acceleration of electrons is indeed increasingly considered as a potential compact substitute of conventional accelerator technology, at least for extreme UV free electron lasers (Grüner et al., 2007; Schlenvoigt et al., 2008; Nakajima 2008). The main problems of this scheme are the stringent requirements on the mono-energeticity of LWFA electrons, and the stability of electron bunches at very high laser accelerated electron energies.

Gruner at al. (2007) studied the possibility to develop table-tops XFELs. They first studied a proof-of-principle scenario at relatively low electron energies, where space-charge effects play a dominant role leading to a linear energy chirp. The situation of the proposed table-top X-FEL (TT-XFEL) is different. To reach a wavelength of $\lambda = 0.25$ nm, an electron energy of 1.74 GeV is needed in case of a period of $\lambda_0 = 5$ mm. Space charge effects are much weaker here. For this less demanding situation they have confirmed with four different simulation codes that above 1 GeV, with the same parameters as in the extreme case given above, Coulomb-explosion leads to a projected energy chirp of below 0.3% and a bunch elongation with a factor below 1.1. Experimentally the most demanding constraint is that the electron (slice) energy spread should be as small as 0.1%. For the authors, this goal seems to be within reach.

Without the effect of wakefields GENESIS simulations have shown that this TT-XFEL scenario with an undulator length of only 5 m yields 8×10^{11} photons/bunch within ~ 4 fs and 0.2% bandwidth, a divergence of 10 μrad, and a beam size of 20μm. However, the wakefields become the dominant degrading effect as the required undulator length is larger. But since there is no initial space-charge-induced energy chirp, one must find another method for compensating the wakefield-induced energy variation. A suitable method for compensating the wakefields for the TT-XFEL could be tapering, i.e., varying the undulator period along the undulator. Due to the fact that the undulator parameter K is smaller than unity, tapering via K, i.e., by gap variation, could only be used as fine-tuning.

Schlenvoigt et al. (2008) have demonstrated the first successful combination of a laser-plasma wakefield accelerator, producing 55–75 MeV electron bunches, with an undulator to generate visible synchrotron radiation. By demonstrating the wavelength scaling with energy, and narrow-bandwidth spectra, they showed the potential for ultracompact and versatile laser-based radiation sources from the infrared to X-ray energies. In their set-up, Schlenvoigt et al. focus the light from a 5-TW laser pulse into a 2-mm-wide gas jet. The interaction of the laser with the jet produces a beam of electrons with a peak energy of between 55–75 MeV. Directing this beam into a 1-m-long undulator — which consists of a series of alternating magnets — causes its electrons to wiggle in the transverse direction,

producing light at the red end of the visible spectrum (with wavelength in the range of 950–550 nm). The authors therefore provide the first demonstration of the production of resonant-like synchrotron radiation from a laser-generated electron beam. The results of several runs of their experiment show that the emission wavelength scales with beam energy just as theory predicts, suggesting that the generation of much shorter wavelengths by this approach should be relatively straightforward. By extending the length of the undulator to 3 m, and feeding it with a more energetic beam — such as the 1-GeV, 30-pC beams recently demonstrated in a 3-cm capillary laser-plasma accelerator (Leemans et al., 2006) — it should soon be possible to reach 3 nm in the soft-X-ray range, at a peak brilliance comparable to that of even the largest modern synchrotron radiation sources.

For Nakajima et al. (Nakajima et al. 2008), once the feasibility of a laser-driven soft-X-ray source is achieved, the next step will be to extend this approach to the more ambitious task of constructing an FEL. This process will require the generation of electron beams of extremely high current and small emittance and energy spread, and the construction of a precisely engineered undulator exceeding a hundred meters in length.

3.2 Laser wiggler concepts

A laser-undulator free electron laser has therefore been repeatedly proposed [Sprangle et al. 1992, Dobiasch et al. 1983, Gea-Banacloche 1987, Sprangle et al. 2009], but has remained so far inapplicable. Many authors have indeed shown that the action of a laser field, counter-propagating with respect to the electrons, is basically equivalent to that of the magnetic field in a wiggler, and thus can be used to obtain an FEL effect (Sprangle 2009b ; Dobiasch et al., 1983; Gea-Banachloche et al, 1987 ; Gallardo et al., 1988). However, the strength parameter K depends strongly on the undulator period. Replacing the magnet period of few cm, by a laser wavelength around 1 µm, results in practice in a very low value of K, and hence in low gain, so that a very high number N of oscillations is required. Since the energy dispersion of the electrons has to be smaller than $1/2N$ for the Compton free electron laser effect to be effective in the small signal regime, this scheme would require an absolutely outstanding quality of mono-energeticity, together with an equivalent requirement on the constancy of the laser intensity along the interaction region, and an outstanding emittance – all constraints well beyond the present or foreseeable state of the art. Due to these major issues, the scheme was never seriously considered, up to a recent proposal by Petrillo et al. (Petrillo et al. 2008), who suggest to use a mono-energetic electron beam predicted to arise from LFWA with i) a huge electron peak current, ii) a quasi mono-energetic distribution, iii) an emittance three times smaller than the current state of the art. By shining a high energy, few picosecond, and monomode CO_2 laser, onto the bunch, Petrillo et al. succeed to meet the conditions outlined above, and predict a coherent emission at 1.4 nm, up to saturation, and have dubbed the process an "All Optical Free Electron Laser". They studied the generation of low emittance high current monoenergetic beams from plasma waves driven by ultrashort laser pulses, in view of achieving beam brightness of interest for free-electron laser (FEL) applications. The aim is to show the feasibility of generating nC charged beams carrying peak currents much higher than those attainable with photoinjectors, together with comparable emittances and energy spread, compatibly with typical FEL requirements. They identified two regimes: the first is based on a laser wakefield acceleration plasma driving scheme in a gas jet modulated in

areas of different densities with sharp density gradients. The second regime is the so-called bubble regime, leaving a full electron-free zone behind the driving laser pulse: with this technique peak currents in excess of 100 kA are achievable. They have focused on the first regime, because it seems more promising in terms of beam emittance. Simulations carried out using VORPAL show, in fact, that in the first regime, using a properly density modulated gas jet, it is possible to generate beams at energies of about 30 MeV with peak currents of 20 kA, slice transverse emittances as low as 0.3 mm mrad, and energy spread around 0.4%. These beams achieve very high brightness, definitely above the ultimate performances of photoinjectors, therefore opening a new range of opportunities for FEL applications. The system constituted by the electron beam under the effect of the electromagnetic undulator has been named AOFEL (for all optical free-electron laser).

In a recent article (Sprangle et al. 2009a), Sprangle et al. use the well-known GENESIS code to confirm the scenario, but emphasize the huge technical challenges, with electron energy spread and laser constancy both required of the order of 0.01%.

To summarize, both schemes presented in this Section are extremely interesting in the soft X-ray range around 1 keV. Both require however in a stringent way extremely challenging parameters of mono-energeticity and emittance of the laser-accelerated electron bunches and seem extremely challenging in view of present day electron and laser technologies. To the best of our knowledge, no compact scheme for an XFEL has yet been proposed, robust enough to be adapted to realistic conditions of relativistic electron bunches.

4. Raman XFEL

In this section, a new scheme for an X-ray free electron laser is described: it is based on a Raman process occurring during the interaction between a moderately relativistic bunch of free electrons, and twin intense short pulse lasers interfering to form a transverse standing wave along the electron trajectories. In the high intensity regime of the Kapitza-Dirac effect, the laser ponderomotive potential forces the electrons into a lateral oscillatory motion, resulting in a Raman scattering process. This triggers a parametric process, resulting in the amplification of the Stokes component of the Raman-scattered photons. Experimental operating parameters and implementations are discussed.

4.1 Principle and geometry: Relativistic electrons in a high intensity optical lattice

A totally new approach to create an X-ray laser was recently proposed by Ph. Balcou (Balcou 2010), based on the interaction between a bunch of moderately relativistic electrons, and an optical lattice created by two interfering laser beams. The key issue is to be able to create artificially a new degree of freedom for the electrons, in which case a Raman scattering process can be expected. If one sets up a configuration to maintain the Raman scattering over a certain distance, then a stimulated effect will be switched, leading to exponential amplification of the Raman scattered light, in the extreme UV or X-ray range depending on the Doppler shift.

Let us first consider the typical setup of 90° Thomson scattering of a laser off a relativistic electron bunch, (see Schoenlein et al., 2000). A short pulse, energetic laser impinges at 90°

onto a relativistic electron bunch. Photons and electrons are focused and superpose onto a focal spot of few tens of μm FWHM, thus scattering of X-ray photons along the electron direction. This is a spontaneous scattering process, and the alignment of the X-ray photons along the electron direction is a pure relativistic kinematic effect.
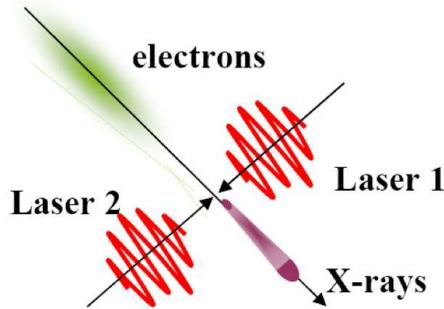

Fig. 8. Proposed 2-beams, 90° scattering.

We now propose to split the incident laser into two identical parts, and send these twin beams in opposite directions, perpendicularly to the electron beam (Fig. 8). In the superposition region, the two beams interfere to form a transverse standing wave. The relativistic electrons interact therefore with an optical lattice, giving rise to an effect known as the strong field Kapitza-Dirac (KD) effect (see section 2 for more details on this effect).

4.2 Electron dynamics: Beam trapping and collective electron modes

Fig. 9 illustrates the proposed scheme, showing the typical behavior of relativistic electrons injected into the transverse optical lattice, in the high intensity regime of the KD effect. The light lattice induces a series of parallel potential wells, aligned along the main electron direction. If the transverse kinetic energy of incident electrons is high, they skip through the potential wells (high emittance / low intensity limit); otherwise, they get trapped into one well, and start oscillating with a characteristic frequency (low emittance/high intensity limit):

$$\Omega = \frac{\sqrt{2}eE_0}{\gamma mc}$$

where E_0 is the laser field of each incident beam, γ the Lorentz factor of electrons of mass m.

This transverse oscillation modifies the photon scattering, splitting the Thomson peak into a doublet of Raman modes. This is illustrated in figure 10, showing the result of an exact numerical calculation of the scattering spectrum of a 10 MeV electron, chosen at random in a 1 μm normalized emittance bunch focused over 30 μm rms, and injected into the transverse light lattice. Individual electrons may oscillate randomly, resulting in a spontaneous Raman scattering.
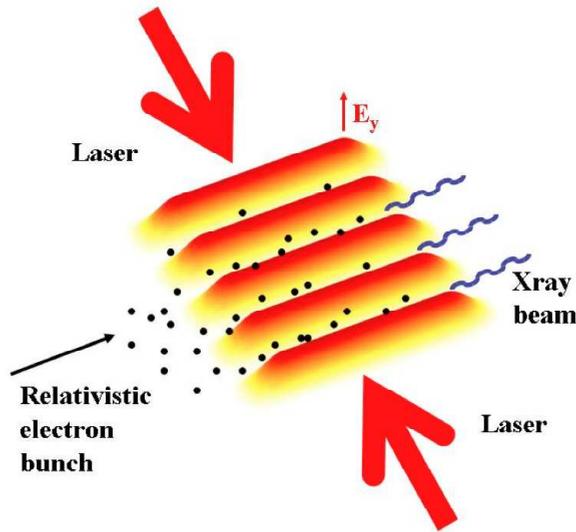
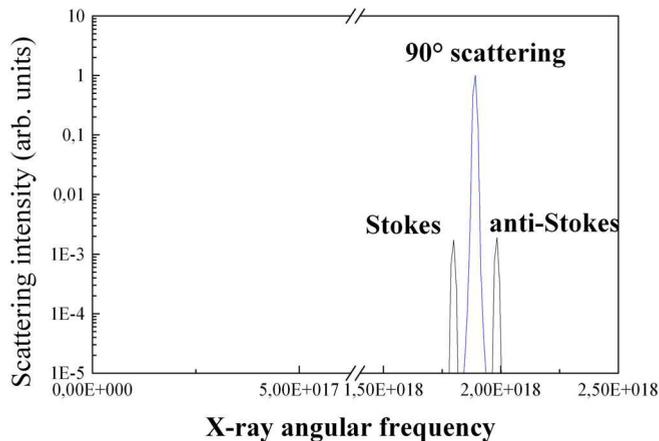Fig. 9. Typical behavior of relativistic electrons injected into the transverse optical lattice.

Fig. 10. Result of an exact numerical calculation of the scattering spectrum of a 10 MeV electron, chosen at random in a 1 µm normalized emittance bunch focused over 30 µm rms, and injected into the transverse light lattice.

If a collective electron oscillatory motion is induced, then one obtains a new kind of oscillatory plasma wave, trapped in the light potential, as illustrated in Figure 11. Excitation of this plasma wave will then lead to a coherent scattering process. The excitation mechanism is currently studied, and can be shown to be similar to the excitation mechanism of standard Free Electron Lasers, by means of a Lorentz force inducing a time-dependent, and tranversely-dependent longitunidal bunching.
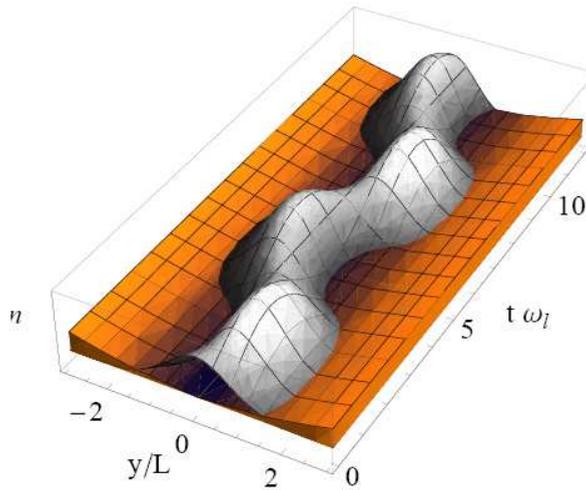
Fig. 11. Oscillatory plasma wave, trapped in the light potential.

The injection of a low emittance, relativistic electron bunch into a transverse light lattice (Fig. 8) in the high intensity regime of the Kapitza-Dirac effect, results therefore in successive phenomena:

1. a trapping of the electron bunch along the stationary wave axis, in the light potential (high intensity optical molasses), as illustrated in Fig. 9;
2. a formation of a new kind of oscillating plasma waves in the light trap (Fig 11) ;
3. a Raman scattering effect of the laser off the oscillating plasma wave (Fig. 10) ;
4. an increased excitation of the plasma wave from the beating between the Raman scattered beam and the laser beams.

These steps are the classical elements required for the growth of a well-known instability, namely, Stimulated Raman Scattering, but with unique characteristics, since the inner degree of freedom is dominated by the transverse oscillations in the light potential, instead of the oscillations in plasma density (which are however taken into account). Whether or not this scattering is efficient enough to yield an actual X-ray laser is the major issue. The two relevant questions are, a) what can be a typical gain length of the instability ?, and b) is it possible to induce and control an interaction over several gain lengths?

Question b) is a very well known issue in plasma-based soft X-ray lasers. In transient collisional schemes, the gain lifetime at any point in the plasma is well below the time needed for a photon to go through the active medium. It is therefore useless to irradiate simultaneously the line focus; on the contrary, irradiation has to be made to follow in time the amplified photons. In (Balcou 2010), it was proposed to use a special optical configuration, called an inhomogeneous wave, in which the pulse energy front is tilted at 45° from the phase fronts, thus irradiating the electron bunch synchronously with its advance. It might also be possible to use a much simpler method, based on the well-known Grazing Incidence Geometry, known as GRIP.

Exploring question a) requires to get estimates for the Raman gain g and gain length. Two separate theoretical models have been developed in that goal. The first model mimics the Compton FEL theory by describing the evolution of the electron bunching, which, in contrast to standard FELs, is not purely longitudinal but also transverse, and oscillating (Fig. 11). The electron density is assumed to be constant, so that the model can be described as a Kinetic Frozen Density model (KFD). It shows that the Stokes mode will undergo exponential amplification, while the anti-Stokes mode is absorbed. The Raman gain is given by:

$$g = \alpha \sqrt{\frac{e^3 n_e E_0}{\varepsilon_0 m^2 c^3 \omega_1}} \; ,$$

where n_e is the electron number density, ω_1 the angular frequency of the X-rays in the Stokes mode, and E_0 the external laser field amplitude, and α a constant of order unity.

A second model has been recently proposed by Prof. Vladimir Tikhonchuk and Dr Igor Andriyash (Andriyash et al. 2011), based on a fluid description of excitation of the electron plasma wave within the bunch. This approach is derived from well-known models to describe Raman instabilities in plasmas. It has the advantage to treat in a unified way the plasma oscillations within the electron bunch, and the collective electron motion in the light potential, for a given electron temperature in the bunch rest frame. This plasma fluid model results in similar gain estimates. The important advantage of this second model is to show that the gain depends strongly on the transverse electron temperature.

4.3 Prospective experimental implementation

Let us see how these two formulas from independent models give estimates of gain lengths in a test case. We consider a medium energy electron beam from Laser Wakefield acceleration in the bubble regime, with the parameters given in the recent article by Davoine et al. (2009): 60 MeV, normalized emittance of 1 mm.mrad, peak current of 25 kA. With a laser intensity of 1.2×10^{18} W/cm^2, the KFD model predicts a gain length of 42 μm, for 43 keV X-ray photons. In identical conditions, the fluid plasma model predicts a similar gain length. The two models agree essentially to predict coherent amplification with very short gain lengths, in typical conditions of electron wakefield acceleration.

Assuming that amplification will saturate for a gain.length product g.L between 6 and 10, that the twin lasers are focused onto a vertical spot of 5 μm FWHM, neglecting for the time the initial latency (time required to start the X-ray wave amplification from noise), and considering typical parameters of Ti:Sa lasers, one obtains estimates of laser energy for the optical undulator of the order of 1 to few Joules – readily available with present-day laser technology.

As a result, analytical estimates show that one can expect to operate a Raman X-ray free electron laser with present-day laser technologies.

It is anticipated that the advantages and drawbacks of a Raman X-ray free electron laser, as compared to the Grüner et al. (2007) or Petrillo et al. (2008) schemes, would be:

- It requires far less stringent parameters in terms of mono-energeticity $\delta\gamma/\gamma$ of the electron bunch. A low value of $\delta\gamma/\gamma$ remains favourable, to avoid spreading the gain over a large inhomogeneous bandwidth, but a value higher than 1% should no longer be a killer. Considering the ongoing progress in Laser Wakefield Acceleration techniques, the interest of coupling LWFA and Raman XFEL approaches appears obvious.
- It requires existing laser technologies. Transverse irradiation also allows active optical elements to control finely the intensity and phase distributions of the twin beams along the interaction region.
- Electrons are trapped and guided transversely, at least in one dimension. Incidentally, a 2-dimensional trap is also possible.
- If a set of working parameters is found, then the whole setup may be upscaled to higher X-ray photons energies by scaling up the laser energy by γ, the electron energy by γ as well, while the output X-ray photon energy scales as γ^2. Coherent X-ray generation beyond few tens of keV seems therefore possible. Moreover, increasing the electron energies to values up to hundreds of MeV or even 1 GeV is possible; therefore the current developments of multi-PetaWatt lasers, and of large projects like ELI (Extreme Light Infrastructure), could make it possible to reach lasing in the γ-ray range in the long term.

The scheme may however also present some drawbacks, as :

- It requires a delicate optical setup, with perfectly controlled twin laser undulator beams;
- It is bound to yield a spectrally rather broad X-ray emission, with a $\delta\omega_1/\omega_1$ of the order of Ω/ω_0 (around 1% expected) ;
- The photon number per pulse is bound to be smaller than with large scale XFELs, due to the larger impact of the recoil phenomenon on the electron energies.

However, this list of advantages and drawbacks is still currently being debated; all these aspects must be studied extensively, with a thorough theoretical investigation, and first experimental tests.

5. Conclusion

Due to the strong demand for bright XFEL facilities and the cost of existing systems, the development of compact XFEL schemes is a very attractive field at the crossroads of particle acceleration physics, optics and plasma physics. Significant progresses have been accomplished in the last few years and new schemes involving the coupling of laser wakefield accelerated electrons with either magnetic or optical wigglers have been proposed. Even if some progresses are being made for each of these schemes, they have very stringent requirements on the accelerated electron beams. Another very promising scheme using counter-propagating lasers to create a ponderomotive potential array in which accelerated electrons will propagate is also under study. Modelling of Raman gain through Particle In Cell simulations is now underway and new kinetic theory results are being compared with 2D PIC simulations in the rest frame of the energetic electron beam and encouraging results have been obtained so far (Andriyash et al., 2012; Andriyash et al., in preparation). A proposition of parameters for an all-optical compact XFEL will first be tested using Particle-In-Cell simulations. The original Kinetic Frozen Density model of (Balcou 2010) is also being improved, especially since it was pointed out that the full effect

of the magnetic field of the X-ray wave should be better taken into account (Zholents and Zolotorev 2011; Balcou 2011). These efforts will lead to an experimental proposal in order to test the obtained theoretical and numerical results.

6. Acknowledgements

7. References

Amiranoff F. et al. (1995), Phys. Rev. Lett., 74 p5220–5223.

Andreev N. E. et al. (1992), JETP Lett., 55 p571.

Andriyash I., Balcou Ph. and Tikhonchuk V.T. (2011), Eur. Phys. J. D, 65, 533.

Andriyash I., Balcou Ph., d'Humières E. and Tikhonchuk V.T. (2012) "Scattering of relativistic electron beam by two counter-propagating laser pulses: a new approach to Raman X-ray amplification", accepted by EPJ – WoC

Andriyash I., d'Humières E., Balcou Ph. and Tikhonchuk V.T. « Particle-In-Cell simulations of Raman X-ray amplification in optical free electron lasers » , in preparation.

Antonsen T. M. et Mora P. (1992), Phys. Rev. Lett., 69 p2204.

Arkhiezer A. I. et Polovin R. V. (1956), Sov. Phys. JEPT, 3 p696–705.

Bacci A. et al. (2006), Phys. Rev. ST Accel. Beams 9, 060704.

Balcou Ph. (2010), Eur. Phys. J. D 59, 525–537.

Balcou Ph. (2011), Eur. Phys. J. D 62, 459-459.

Bloembergen N. et al. (1999), Rev. Mod. Phys. 71, S283.

Bucksbaum Ph. Et al. (1988), Phys. Rev. Lett. 61, 1182.

Carroll F. (2003), Journ. Cell. Biochem. 90, 502–508.

Clayton C. E. et al. (1994). Phys. Plasmas., 1 p1753.

Davoine X. et al. (2009), Phys. Rev. Lett. 102, 065001.

Dobiasch P., Meystre P., Scully M.O. (1983), IEEE J. Quantum Electron. 19, 1812.

Emma P. and LCLS commissioning team (2009), Proceedings of the PAC conference.

Emma P. et al. (2010), Nature Photonics 4, 641 - 647.

Everett M.J. et al. (1994), Nature, 368 p527–529.

Faure J. et al. (2004), Nature, 431 p541.

Faure J. et al. (2006), Nature 444, 737-739.

Fedorov V.M. et al. (1988), App. Phys. Lett. 53, 353.

Freimund D.L., Aflatooni K., Batelaan H. (2001), Nature 413, Issue 6852, 142].

Freund H.P. and Antonsen T.M. (1996), Principles of free-electron lasers, Chapman & Hall.

Fritzler S. et al. (2004), Phys. Rev. Lett., 92 p165006.

Gahn C. et al. (1999), Phys. Rev. Lett., 83 p4772.

Gallardo J.C., et al. (1988), IEEE J. Quantum. Electron. 24, 1557.

Gea-Banacloche J. et al. (1987), IEEE J. Quantum. Electron. 23, 1558.

Geddes C. G. R. et al. (2004), Nature, 431 p538.

Gibbon P. (2005) "Short pulse laser interactions with matter. An Introduciton" Imperial College Press, London.

Grüner F. et al. (2007), APB 86, 431.

Hafz N.A.M. et al. (2008) Nature Phot. 2, 571-577.

Hartemann (2000), Astrophys. Journ. Supp. Series 127, 347.

Hidding B. et al. (2006), Phys. Rev. Lett., 96 p105004.

Hosokai T. et al. (2003), Phys. Rev. E, 67 p036407.

Jaeglé P. (2006), Coherent sources of XUV radiation (Springer Verlag, Berlin).

Joshi C., et al. (1981), Phys. Rev. Lett., 60 p1298.

Kapitza P.L., Dirac P.A.M. (1933), Proc. Cambridge Philos. Soc. 29, 297.

Katsouleas T. and Mori W.B. (1988), Phys. Rev. Lett., 61 p90–93.

Kibble T.W.B. (1968), Phys. Rev. 150, 1060.

Kitagawa Y. et al. (1992), Phys. Rev. Lett., 68 p48.

Lau et al. (2003), Phys. Plasmas, Vol. 10, No. 5.

Leemans W.P. et al. (2004), Phys. of Plasmas, 11 p2899–2906.

Leemans, W. et al. (2006), Nature phys. 2, 696.

Liu J.S. et al. (2011), Phys. Rev. Lett. 107, 035001.

Loew G.A. and Talman A. (1983), SLAC-PUB-3221, Sec. 2(Sep.).

Lu W. et al. (2007), Phys. Rev. ST-AB 10, 061301.

Lundh O. et al. (2011), Nature Physics 7, 219.

Malka G., Lefebvre E., and Miquel J.L. (1997) Phys. Rev. Lett. 78, 3314-3317.

Malka V. et al. (2001), Physics of Plasmas, 8 p2605–2608.

Malka V. et al. (2002), Science, 298 p1596–1600.

Mangles S. et al. (2004), Nature, 431 p535.

Miura E. et al. (2005), Appl. Phys. Lett., 86 p25150.

Nakajima K. (2008), Nature Phys. 4, 92.

Petrillo V., Serafini L., and P. Tomassini (2008), Phys. Rev. Sel. Top. Acc. Beams 11, 070703.

Pollock B.B. et al. (2011), Phys. Rev. Lett. 107, 045001.

Pukhov A. and Meyer-ter-Vehn J. (2002), Appl. Phys. B, 74 p355.

Rosenzweig J.B. (1988), Phys. Rev. A, 38 p3634.

Rousse A. et al. (2001), Rev. Mod. Phys. 73, 17.

Schlenvoigt H.P. et al. (2008), Nature Phys. 4, 130.

Schoenlein R.W. et al (1996), Science, 274, 236.

Schoenlein R.W. et al (2000), Science, 287, 2237.

Schoenlein R.W. et al. (2000), Appl. Phys. B, 71, 1

Sprangle P., Esarey E., Krall J. et Joyce G. (1992), Phys. Rev. Lett., 69 p2200.

Sprangle P., Hafizi B., Peñano J.R. (2009), Phys. Rev. Sel. Top. Acc. Beams 12, 050702.

Sprangle P. (2009), JAP 50, 2652 12, 050702.

Strickland D. and Mourou G. (1985), Opt. Comm., 56 p219–221.

Tajima T. and Dawson J.M. (1979) "Laser electron accelerator" Phys. Rev. Lett. 43, 267-270.

Tsung F.S. et al. (2004), Phys. Rev. Lett., 93 p185002.

Ultrafast Phenomena proceedings (1992- 2002), Springer Ser. Chem. Phys. Vol. 55, 60, 62, 63, and 66 (Springer, Berlin).

Wilson P.B. (2008), Rev. Acc. Science Tech., 1, 7.
Winick H. et al. (1981), Physics Today 34, 50.
Zewail A.H. (2000), J. Phys. Chem. A 104, 5660.
Zholents A. and Zolotorev M. (2011), Eur. Phys. J. D 62, 457 (2011).
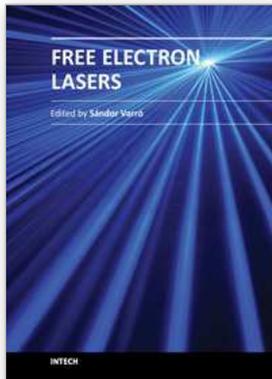
Free Electron Lasers

Edited by Dr. Sandor Varro

Free Electron Lasers consists of 10 chapters, which refer to fundamentals and design of various free electron laser systems, from the infrared to the xuv wavelength regimes. In addition to making a comparison with conventional lasers, a couple of special topics concerning near-field and cavity electrodynamics, compact and table-top arrangements and strong radiation induced exotic states of matter are analyzed as well. The control and diagnostics of such devices and radiation safety issues are also discussed. Free Electron Lasers provides a selection of research results on these special sources of radiation, concerning basic principles, applications and some interesting new ideas of current interest.

How to reference

In order to correctly reference this scholarly work, feel free to copy and paste the following:

Emmanuel d'Humières and Philippe Balcou (2012). Compact XFEL Schemes, Free Electron Lasers, Dr. Sandor Varro (Ed.), ISBN: 978-953-51-0279-3, InTech, Available from: http://www.intechopen.com/books/free-electron-lasers/compact-x-ray-free-electron-laser-schemes

INTECH
open science | open minds